

## Dynamical Modeling and Identification of a GnRH neuron <sup>\*</sup>

Dávid Csercsik <sup>\*</sup> Gábor Szederkényi <sup>\*</sup> Katalin M. Hangos <sup>\*</sup>  
Imre Farkas <sup>\*\*</sup>

<sup>\*</sup> *Process Control Research Group, Systems and Control Laboratory, Computer and Automation Research Institute, HAS, Budapest Hungary*  
csercsik@scl.sztaki.hu, szeder@scl.sztaki.hu, hangos@scl.sztaki.hu

<sup>\*\*</sup> *Department of Endocrine Neurobiology, Institute of Experimental Medicine, HAS, Budapest, Hungary* farkas@koki.hu

---

**Abstract:** GnRH neurons, as key elements of the reproductive neuroendocrine system, have important central regulating role in the dynamics of the hormonal cycle. A Hodgkin-Huxley type neural model is proposed in this paper, that takes into account up-to-date biological literature data related to ion channels. The proposed neuron model is highly nonlinear in parameters and the evaluation of the objective function is computationally expensive, therefore the asynchronous parallel pattern search (APPS) procedure has been used for identification. The model with high number of estimated parameters provides a qualitatively good fit of both voltage clamp and current clamp traces.

*Keywords:* Neural dynamics, Dynamic modelling, Identification, Nonlinear systems

---

### 1. INTRODUCTION

The first fundamental mathematical model of the reproductive neuroendocrine system that aimed to describe the hormone levels during the menstrual cycle was developed by Harris (2001); Harris et al. (2006). This model was used for further research by several authors, e.g. Reinecke and Deuffhard (2007). An appropriate predictive model of this interesting system, describing the main biological phenomena and interactions, would have a significant importance in theoretical and clinical field as follows.

- A better understanding, and further insight could be provided into mechanisms, that underlie the dynamics of the hormonal system.
- The effect of possible new hormonal drugs (incl. hormonal contraceptives) could be pre-tested before in-vitro, animal and clinical experiments and assays.
- Proposals could be made for the treatment and therapy of various hormonal diseases and disorders. This is a challenging and unusual task, because pulsatile administration of e.g. GnRH is desired in several cases, see Tan et al. (1996); Zinaman et al. (1995).

To increase the clinical relevance of such models, one has to use sub-models based on as up-to-date biological information as available, and reduce the role of empirical and phenomenological approaches.

One part of the reproductive neuroendocrine system, where this approach offers a great potential, is the GnRH pulse generator. This neuronal pulse generator governs the central control of reproduction in vertebrates. The GnRH

pulse generator controls the activity of hypothalamic neuroendocrine cells that secrete GnRH in a pulsatile way, closely associated with concurrent increases in multiunit electrical activity in the mediobasal hypothalamus (MUA volleys) (See Knobil (1980, 1988)).

*The role of GnRH neurons* The pulsatile release of GnRH is driven by the intrinsic activity of GnRH neurons, which is characterized by bursts and prolonged episodes of repetitive action potentials correlated with oscillatory increases in intracellular  $Ca^{2+}$ .

Several in vitro experiments have shown that changes in cytosolic  $Ca^{2+}$  concentration determine the secretory pattern of GnRH - see Stojilkovic et al. (1994) -, underlining that  $Ca^{2+}$  plays a central role in the signal transduction processes that lead to exocytosis. Furthermore, as described by Krsmanovic et al. (1992), GnRH secretion from perfused GT-1 and hypothalamic cells is reduced by L-type  $Ca^{2+}$  channel inhibitors and augmented by activation of voltage-gated  $Ca^{2+}$  channels. These results underline the importance of modeling  $Ca^{2+}$  currents, because the model is presumed to be later extended with the description of intracellular  $Ca^{2+}$  levels to describe hormone secretion.

*Significance and aim* The models of the GnRH pulse generator, which can be found in literature nowadays, use generalized and very simple neuron models and networks. Furthermore, they are neither based on the known membrane properties of GnRH neurons, nor are able to describe the effect of ovary hormones - see Brown et al. (1994). Nevertheless, these results can provide interesting insights into pulsatility and synchronization as described by Khadra and Li (2006); Gordan et al. (1998).

---

<sup>\*</sup> This work was supported by the Hungarian Research Fund OTKA through grant K67625. Gábor Szederkényi is a grantee of the Bolyai scholarship of the Hungarian Academy of Sciences.

With the application of cell marking based on the green fluorescent protein (GFP) and transgenic mice, the targeted measurements and experiments on GnRH neurons became available, see Herbison et al. (2001); Suter et al. (2000). Another possibility is the application of so called "immortalized" GnRH neurons, as described by Mellon et al. (1990). The new biological data originating from these measurements, together with the new (or appropriately reformulated and integrated) approaches in the neoclassical computational neuroscience by Izhikevich (2000, 2005) offer promising possibilities in the field of modeling and identification of GnRH neurons and the GnRH pulse generator network.

The work reported in this paper is intended to be the first step in a bottom-up procedure which aims to build a hierarchical model of the GnRH pulse generator that includes the effects of ovarian hormones. In order to reach this aim, GFP-based patch clamp recordings were done on mice GnRH neurons at the Institute of Experimental Medicine (KOKI). The measured data are used to identify a Hodgkin and Huxley (1952) type conductance-based model of membrane dynamics.

## 2. MATERIALS AND METHODS

The measurements, the model development and the parameter estimation method are described in this section.

### 2.1 Measurements

*Obtaining and preparing samples* Mouse brain was used for obtaining GnRH neurons for measurements. The mouse was decapitated, and the brain was rapidly removed and placed in ice-cold artificial cerebrospinal fluid (ACSF) oxygenated with 95%  $O_2$ -5%  $CO_2$  mixture. Brains were blocked and glued to the chilled stage of a vibratome, and 250-micrometer-thick coronal slices containing the medial septum through to the preoptic area were cut. The slices were then incubated at room temperature for 1 hour in oxygenated ACSF consisting of (in mM): 135 NaCl, 3.5 KCl, 26 NaHCO<sub>3</sub>, 10 D-glucose, 1.25 NaH<sub>2</sub>PO<sub>4</sub>, 1.2 MgSO<sub>4</sub>, 2.5 CaCl<sub>2</sub>, pH 7.3.

*Whole-cell recording of GnRH neurons* Slices were transferred to the recording chamber, held submerged, and continuously superfused with oxygenized ACSF. All recordings were made at 33°C.

In order to visualize GnRH neurons in the brain slices, GnRH-enhanced green fluorescent protein (GnRH-GFP) transgenic mice were chosen in which the GnRH promoter drives selective GFP expression in the majority of GnRH neurons.

The electrodes were filled with intracellular solution (in mM): 140 KCl, 10 HEPES, 5 EGTA, 0.1 CaCl<sub>2</sub>, 4 MgATP, 0.4 NaATP, pH 7.3 with NaOH. Resistance of patch electrodes was 2-3 MΩ. Holding potential was -70 mV, near the average resting potential of the GnRH cells. Pipette offset potential, series resistance and capacitance were compensated before recording.

### 2.2 Model development

Using literature data on the ion channels of the GnRH neuron and properties of ion channels, a simple GnRH neuron-model can be developed and identified involving further literature data, voltage clamp and current clamp measurements. Measurement data were available in the form of whole cell patch-clamp recordings.

*The suggested model framework of single cell models* A single compartment Hodgkin-Huxley (HH) type model - see Hodgkin and Huxley (1952) - is suggested, which can be extended to a multicompartmental structure, if needed, for the description of bursting. The main benefits of this model class are the following.

- Each ion channel is represented by an element of the model (conductance), so different ion channels can be taken into account separately, and in a *modular* way. This structure allows the integration of most available literature data into the model.
- The properties of specific ionic currents *can be measured separately* via voltage clamp (reversal potential-based) methods combined with pharmacological (TTX, TEA, etc. based) methods. These types of measurements can gather data corresponding to specific elements of the model. This implies the benefit of the opportunity, that various elements of the model can be identified separately, using different parameter estimation methods, if needed.
- Because the different ion channels are described by different elements of the model, the model can be extended with equations describing the effect of estradiol, acting on specific ion channels.

*Elements of the model* According to the literature data, previous results point to the existence of the following conductance elements in the GnRH neuron:

- Na<sup>+</sup> channel: According to Bosama (1993); Kusano et al. (1995), a simple voltage gated inward rectifier Na<sup>+</sup> channel can be assumed, with standard characteristics. The current related to this channel will be denoted by  $I_{Na1}$ .
- Based on the results of Kusano et al. (1995); Constantin and Charles (2001); Sim et al. (2001); Bosama (1993); Herbison et al. (2001), a voltage gated transient or rapidly activating/ inactivating K<sup>+</sup> conductance is also taken into account, responsible for the rapid, transient component of the outward K<sup>+</sup> current ( $I_{K1}$ ).
- A voltage gated delayed outward rectifier K<sup>+</sup> channel can be assumed, which contributes to the more slowly activating, sustained component of the outward K<sup>+</sup> current ( $I_{K2}$ ) - see Kusano et al. (1995); Constantin and Charles (2001); Sim et al. (2001); Bosama (1993); Herbison et al. (2001).
- According to Kato et al. (2003); Van Goor et al. (1999); Herbison et al. (2001), a low voltage gated (T-type) Ca<sup>2+</sup> channel can be assumed, which is activated in earlier phases of depolarization ( $I_{Ca1}$ ).
- Furthermore, based on Watanabe et al. (2004); Kato et al. (2003) we assume a high voltage gated Ca<sup>2+</sup> channel representing R and N type conductances ( $I_{Ca2}$ ).

- Lastly, a high voltage gated, long-lasting current (L-type)  $\text{Ca}^{2+}$  channel is modelled ( $I_{Ca3}$ ) - see Krsmanovic et al. (1992); Van Goor et al. (1999).
- In addition, a leakage current with constant conductance is also taken into account ( $I_L$ ).

The **equivalent electric circuit** of a one-compartment GnRH neuron model with all the above conductances is shown in Fig. 1.

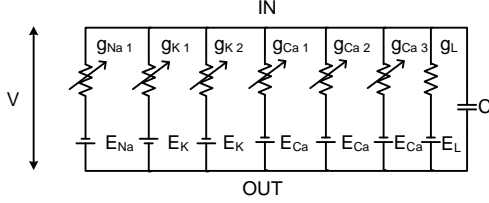


Fig. 1. Parallel conductance model, with conductances representing different ion channels

Literature data of qualitative features and parameters related to some of the above ion channels can be found in Rehm and Tempel (1991); Talavera and Nilius (2006); Kato et al. (2003).

*Model equations* The model depicted in Fig. 1 can be described by the following equations:

$$\frac{dV}{dt} = -\frac{1}{C}(I_{Na1} + I_{K1} + I_{K2} + I_{Ca1} + I_{Ca2} + I_{Ca3} + I_L) + \frac{1}{C}I_{ex} \quad (1)$$

$$\frac{dm_i}{dt} = (m_{i\infty} - m_i)/\tau_{mi}, \quad \frac{dh_i}{dt} = (h_{i\infty} - h_i)/\tau_{hi} \quad (2)$$

where  $V$  is the the membrane voltage,  $C$  is the membrane capacitance,  $I_{Na1}$  denotes the sodium current,  $I_{K_i}$  denotes the various potassium currents,  $I_{Ca_i}$  stands for the calcium currents,  $I_L$  for the leakage. The  $m_i$  and  $h_i$  variables are the activation and inactivation variables of the corresponding currents.  $m_{i\infty}$ ,  $h_{i\infty}$  and  $\tau_{mi}/\tau_{hi}$  denote the steady-state activation and inactivation functions, and the voltage dependent time constants of activation and inactivation variables, which are nonlinear Boltzmann and Gauss -like functions of the membrane potential:

$$a_{\infty i} = \frac{1}{1 + e^{\frac{V_{half_{ai}} - V}{K_{ai}}}}$$

$$a \in \{m, h\}, \quad i \in \{1, 2, 3, 4, 5, 6\}, \quad K_{mi} > 0, K_{hi} < 0 \quad \forall i$$

$$\tau_{ai} = C_{base_{ai}} + C_{amp_{ai}} e^{\frac{-(V_{max_{ai}} - V)^2}{\sigma_{ai}^2}} \quad (3)$$

Finally,  $I_{ex}$  refers to the external injected current, and the indices refer to:  $i = 1 - I_{Na1}$ ,  $i = 2 - I_{K1}$ ,  $i = 3 - I_{K2}$ ,  $i = 4 - I_{Ca1}$ ,  $i = 5 - I_{Ca2}$ ,  $i = 6 - I_{Ca3}$ . The currents of ionic channels are given by

$$\begin{aligned} I_{Na1} &= \bar{g}_{Na1} m_1^3 h_1^2 (V - E_{Na}), & I_{K1} &= \bar{g}_{K1} m_2 h_2^2 (V - E_K) \\ I_{K2} &= \bar{g}_{K2} m_3 h_3 (V - E_K), & I_{Ca1} &= \bar{g}_{Ca1} m_4 h_4 (V - E_{Ca}) \\ I_{Ca2} &= \bar{g}_{Ca2} m_5 h_5 (V - E_{Ca}), & I_{Ca3} &= \bar{g}_{Ca3} m_6 h_6 (V - E_{Ca}) \\ I_L &= \bar{g}_L (V - E_L) \end{aligned} \quad (4)$$

where the  $E_{Na}$ ,  $E_K$ ,  $E_{Ca}$  and  $E_L$  denote the reversal potentials of the corresponding ions and the leakage current.

### 2.3 Voltage and current clamp recordings

The identification was based on both voltage clamp and current clamp measurements. In the case of voltage clamp, the term  $I_{ex}$  in eq. (1) was defined to force the clamping voltage to the membrane:  $I_{ex} = p(V_{clamp} - V)$ . Considering this modification, with a  $p$  big enough, the desired voltage step could be simulated with the same model used later for current clamp simulations.

This basic membrane dynamics-model is considered to be acceptable, if it approximates available measurement data quantitatively well. This observation is used to formulate an appropriate objective function for the parameter estimation.

*Voltage Clamp (VC) without prepulse* The manipulated external input to the system was the clamping voltage  $V_{clamp}$ . Square signals of different amplitudes were used as inputs. The parameters of the voltage steps were the following: The holding potential was  $-70\text{mV}$ , and voltage steps of  $40$  to  $-20$  mV were applied with duration of  $30$  ms starting at  $10$  ms of the recording. The measured output was the total output membrane current:

$$I_{out} = I_{Na1} + I_{K1} + I_{K2} + I_{Ca1} + I_{Ca2} + I_{Ca3} + I_L$$

The objective function of the estimation was the standard two-norm of the difference between the measured and computed output currents for the three measurements, i.e.

$$W(\theta)_{VC} = \frac{1}{N} \sum_i \|I_{out,i}^m - I_{out,i}^s\|_2$$

where  $\theta$  is the estimated parameter vector, and  $I_{out,i}^m$  and  $I_{out,i}^s$  denote the measured and model computed (simulated) total output current (as a discrete time sequence) for the  $i$ th measurement, respectively. Furthermore,  $N$  is the number of data points. The sampling time of the VC measurements was  $0.1$  ms.

*Voltage Clamp (VC) with prepulse* The setup in this case was the same as in the case without prepulse, but the clamping voltage included a  $-100$  mV prepulse with duration of  $9.2$  ms starting at  $0.8$  ms.

*Current Clamp (CC)* The manipulated external input to the system was the excitation current  $I_{ex}$ . The holding current was  $0$  pA. A square signal of  $50$  pA of amplitude with duration of  $200$  ms starting at  $50$  ms was used as input. The measured output was the membrane voltage  $V$ . In this case, the objective function takes the form:

$$W(\theta)_{CC} = \frac{1}{N} \|V_{out,1}^m - V_{out,1}^s\|_2$$

where the notations refer to the measured and estimated signals as in the case of VC.

The overall value of the objective function is calculated as the sum of VC and CC objective functions, i.e.  $W(\theta) = W(\theta)_{CC} + W(\theta)_{VC}$ . The sampling time of the CC measurements was  $0.5$  ms.

### 2.4 Parameter estimation method

The estimated parameters were the membrane capacitance  $C$  in (1), the maximal conductances  $\bar{g}_i$  where  $i \in$

$\{Na1, K1, K2, Ca1, Ca2, Ca3, L\}$ , in Eqs (4), and the activation parameters  $V_{half}, K, C_{base}, C_{amp}, \sigma, V_{max}$  in (3). The parameter estimation procedure minimizes the objective functions defined in the previous section as a function of the parameters to be estimated, i.e. an optimization-based estimation procedure is used.

*Initial values for the optimization* Before applying the optimization algorithm, intuitive rough-tuning of the activation parameters (parameters of the Boltzmann and Gauss functions) and conductance values was performed to capture some important features of the neural behavior (e.g. the model should fire action potentials as response to the exciting current, the firing frequency, the local maxima after the appearance of the exciting current should be similar). This preparation proved to be necessary for convergence to an acceptable optimum.

This laborous procedure was mainly based on qualitative considerations. The intuitive initialization of activation parameters was based on decomposition of the CC trace. The considered parts of the CC trace are shown in Fig 4. This means that from different parts of the CC trace, the initial values of different parameters were guessed.

- *Resting potential*: determined by the leak, delayed rectifier ( $I_{K2}$ ), low threshold  $Ca$  ( $Ca_1$ ) conductances and steady-state parameters ( $m_\infty, h_\infty$ ).
- *Injected current-induced depolarization* is altered by  $C$  and the  $K, Na, Ca_1$  currents
- *Upstroke of APs* influenced by  $Na$  current
- *Downstroke of AP* is determined mainly by  $Na, K$  currents
- *Interspike intervals* are influenced by  $K_1, K_2, Ca_1$ , Leak currents

The following phenomena have to be explained by choosing appropriate initial values of the parameters.

- In the case of voltage step measurements, the negative spike was much greater in the case of lower values of the voltage step (from -70 to -20 mV) - see figures 2 and 3. Based on simulation experiments, it was assumed that this phenomena is not caused by inactivation of  $Na$  current in higher voltage ranges (because it is considered as a slower process compared to activation), but the significant fast activation of overlapping A type  $K$  currents in the higher voltage ranges.
- The difference between the prepulse-free and prepulse VC measurements was quite substantial. In this case the de-inactivation (recovery) parameters had to be analyzed.

The determination of suitable initial values was decomposed into two phases. First, the activation parameters were chosen and then, the maximal channel conductances were estimated from VC and CC data. After a result for conductance values, the activation parameters were further tuned via numerical optimization.

*Optimization algorithm* Since the activation variables can not be measured, a simulation based minimization of the objective function was performed. Because of the model nonlinearity, the objective function value can be a complicated function of the estimated parameters. More-

over, the precise simulation of the system dynamics for a given parameter set is computationally quite demanding, i.e. a few hundred evaluations of the objective function takes a couple of hours on a typical desktop PC. This also means that avoiding the numerical approximation of the gradients of the objective function was desirable in our case. A promising alternative is the freely available Asynchronous Parallel Pattern Search (APPS) algorithm for parameter estimation. As described by Hough et al. (2000), the parallel pattern search (PPS) is a useful tool for derivative-free optimization where the number of variables is not large (about fifty or less) and the objective function is expensive to evaluate.

As described by Kolda (2005), the APPS algorithm is an asynchronous extension of the PPS method that efficiently handles situations when the individual objective function evaluations may take significantly different time intervals and therefore it is very suitable to be implemented in a parallel or grid environment. Furthermore, recent implementations of the APPS method handle bound and linear constraints on the parameters. The global convergence of APPS under standard assumptions is also proved by Kolda and Torczon (2004).

### 3. RESULTS AND DISCUSSION

As a result of the initializing and the algorithm a parameter set was found (see in Table 1), which provided good approximation of several qualitative features (e.g. firing only during current injected, firing frequency, resting potential).

C	$\bar{g}_{Na1}$	$\bar{g}_{K1}$	$\bar{g}_{K2}$	$\bar{g}_{Ca1}$	$\bar{g}_{Ca2}$	$\bar{g}_{Ca3}$	$\bar{g}_L$
5.3	160	62	75	53	16	6	0.5

where [C]=pF and [g]=nS.

act. variable	$V_{half}$	$K$	$V_{max}$	$\sigma$	$C_{amp}$	$C_{base}$
$m_1$	-35.5	3.7	-43	25	0.42	0.13
$h_1$	-46	-6	-57	22	8.2	0.7
$m_2$	-28	10.5	-78	34	8.7	0.8
$h_2$	-60	-7	-23	24	6.9	9
$m_3$	-0.5	13.49	-50	40	5.7	3.5
$h_3$	-66.7	-7.5	-40	25	140	200
$m_4$	-43	5	-40	42	70	92
$h_4$	-74	-4	-65	19	20.5	0.3
$m_5$	0	10	-34	33	0.4	0.5
$h_5$	-37	-11.5	-67	33	52	22
$m_6$	1	9	-44	28	0.9	0.6
$h_6$	-34	-11.5	-70	45	50	110

Table 1

where  $[V_{half}]$ =mV  $[V_{max}]$ =mV  $[C_{amp}]$ =ms  $[C_{base}]$ =ms

It has to be noted that the simulations were started from the initial voltage corresponding to the observed resting potential, and all activation values were set to their steady-state values, corresponding to this voltage.

The measured and simulated results of the voltage clamp measurements are depicted in Figs. 2 and 3. The measured and simulated results of current clamp are depicted in Fig. 4.

As it can be seen in Figs. 2 and 3, the model performs better in the high voltage range in the case of VC. It is also visible from the figures, that the model can not fully

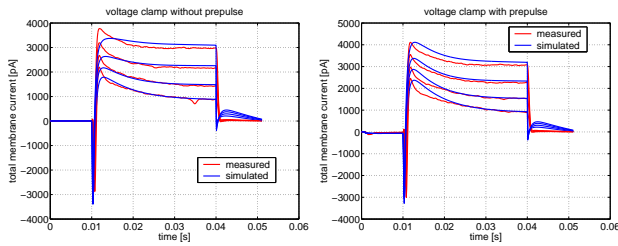


Fig. 2. Measured and simulated membrane currents in the case of VC without and with prepulse in the medium voltage range: red line - measured, blue - simulated

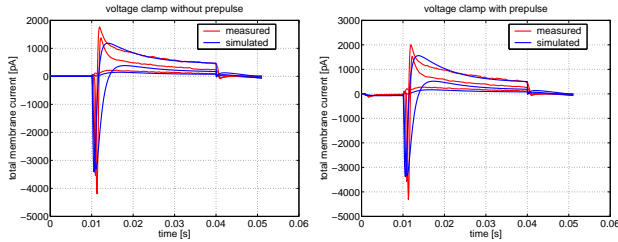


Fig. 3. Measured and simulated membrane currents in the case of VC without and with prepulse in the low voltage range

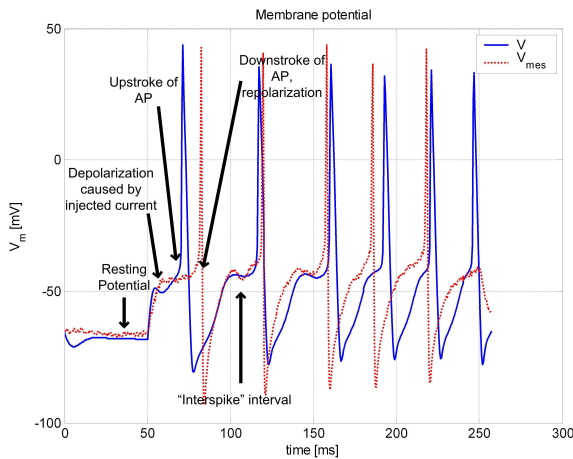


Fig. 4. Measured and simulated membrane voltage in the case of CC

reproduce the high-frequency components in the CC and VC traces. Because of the noise and postsynaptic currents this is acceptable, but regarding the fast currents, the model can still be improved. This model error can be related to the smaller de- and repolarization amplitudes during the AP.

The simulated currents during firing are depicted in Fig. 5. It can be seen that according to the simulation results with the identified model, the action potential upstroke is dominantly determined by the sodium current, while the T-type *Ca* current plays a role in the depolarization before the AP and in the interspike intervals. The amplitude of the T-type current during AP is not comparable to the R-type current because of the low inactivation threshold, in contrast it is very important in the depolarization phase. Furthermore the amplitude and the qualitative features of the *Ca* currents during VC simulation (not depicted here)

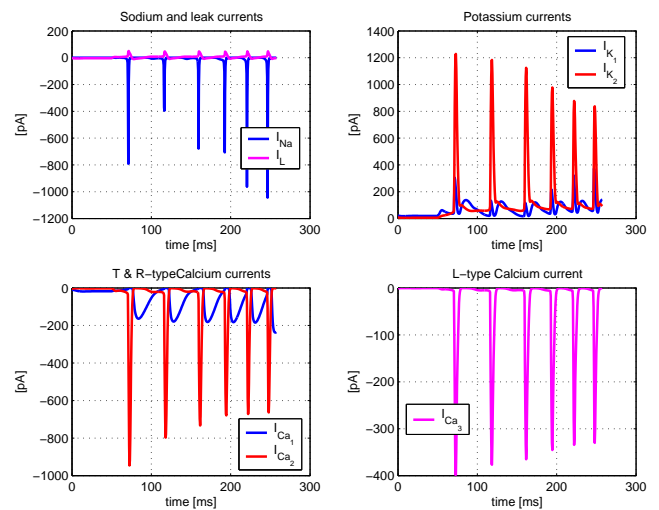


Fig. 5. Simulated membrane currents in the case of CC are in good agreement with the results of Watanabe et al. (2004); Kato et al. (2003). Figure 5 furthermore suggests, that the fast and the delayed rectifier potassium currents determine the downstroke of action potentials together, and the delayed rectifier current plays also significant role in the interspike intervals, affecting the firing frequency.

A phenomena, which indicates a further model error, is the tail current in the VC simulations after 40 ms. These currents can not be observed in the measurements - in the simulations they can be related to the delayed-rectifier conductance.

#### 4. CONCLUSIONS AND FUTURE WORK

In this article, a Hodgkin-Huxley type model of the GnRH neuron and its parameter estimation procedure was proposed. An important aim during the work was to incorporate up-to-date biological literature data into the model. The initial values for parameter estimation were determined using known results and prior knowledge about the modeled system. It is emphasized, that the used mathematical model shows acceptable fit to the measurements with the same estimated parameter values both in the case of VC and CC that can be rarely found in the literature, although a high number of parameters had to be tuned to reach the appropriate behavior. This suggests that the model is possibly overparametrized. The resulting parameter set showed great sensitivity to the initial conditions of the optimization, which were tuned using qualitative considerations.

In the future, we intend to develop an at least semi automatized identification method which would be based on both voltage and current clamp recordings. Since the objective function seems to be quite fragmented as a function of the parameters, the appropriate re-parametrization of the model and/or the application of other parameter estimation methods that do not require the simulation of continuous-time models may be necessary in the future.

#### ACKNOWLEDGEMENTS

GnRH-enhanced green fluorescent protein (GnRH-GFP) transgenic mice were a kind gift by Dr. Suzanne Moenter.

## REFERENCES

- Bosama, M. (1993). Ion channel properties and episodic activity in isolated immortalized gonadotropin-releasing hormone (GnRH) neurons. *Journal of Membrane Biology*, 136, 85–96.
- Brown, D., Herbison, A., Robinson, J., Marrs, R., and Leng, G. (1994). Modelling the lutenizing hormone-releasing hormone pulse generator. *Neuroscience*, 63, 869–879.
- Constantin, J. and Charles, A. (2001). Modulation of  $Ca^{2+}$  signaling by  $K^+$  channels in a hypothalamic neuronal cell line (GT-1). *Journal of Neurophysiology*, 85, 295–304.
- Gordan, J., Attardi, B., and Pfaff, D. (1998). Mathematical exploration of pulsatility in cultured gonadotropin-releasing hormone neurons. *Neuroendocrinology*, 67, 2–17.
- Harris, L., Schlosser, P.M., and Selgrade, J.F. (2006). Multiple stable periodic solutions in a model for hormonal control of the menstrual cycle. *Bulletin of Mathematical Biology*, 65, 157–173.
- Harris, L. (2001). *Differential equation models for the hormonal regulation of the menstrual cycle*. PhD thesis, North Carolina State University, [www.lib.ncsu.edu/theses/available/etd-04222002-153727/unrestricted/etd.pdf](http://www.lib.ncsu.edu/theses/available/etd-04222002-153727/unrestricted/etd.pdf).
- Herbison, A., Pape, J., Simonian, S., Skynner, M., and Sim, J. (2001). Molecular and cellular properties of GnRH neurons revealed through transgenics in mouse. *Molecular and Cellular Endocrinology*, 185, 185–194.
- Hodgkin, A. and Huxley, A. (1952). A quantitative description of membrane current and application to conduction and excitation in nerve. *Journal of Physiology*, 117, 500–544.
- Hough, P.D., Kolda, T.G., and Torczon, V.J. (2000). Asynchronous parallel pattern search for nonlinear optimization. *SIAM Journal on Scientific Computing*, 23, 134–156.
- Izhikevich, E. (2000). Neural excitability, spiking and bursting. *International Journal of Bifurcation and Chaos*, 10, 1171–1266.
- Izhikevich, E. (2005). *Dynamical Systems in Neuroscience*. The MIT Press, 999 Riverview Drive Suite 208 Totowa New Jersey 07512.
- Kato, M., Ui-Tei, K., Watanabe, M., and Sakuma, Y. (2003). Characterization of voltage-gated calcium currents in gonadotropin-releasing hormone neurons tagged with green fluorescent protein in rats. *Endocrinology*, 144, 5118–5125.
- Khadra, A. and Li, Y. (2006). A model for the pulsatile secretion of gonadotropin-releasing hormone from synchronized hypothalamic neurons. *Biophysical Journal*, 91, 74–83.
- Knobil, E. (1980). The neuroendocrine control of the menstrual cycle. *Hormone Research*, 36, 53–88.
- Knobil, E. (1988). The hypothalamic gonadotropin hormone releasing hormone (GnRH) pulse generator in the rhesus monkey and its neuroendocrine control. *Human Reproduction*, 3, 29–31.
- Kolda, T.G. (2005). Revisiting asynchronous parallel pattern search for nonlinear optimization. *SIAM J. Optim.*, 16, 563–586.
- Kolda, T. and Torczon, V. (2004). On the convergence of asynchronous parallel pattern search. *SIAM J. Optim.*, 14, 939–964.
- Krsmanovic, L., Stojilkovic, S., Merelli, F., Dufour, S., Virmani, M., and Catt, K. (1992). Calcium signaling and episodic secretion of gonadotropin-releasing hormone in hypothalamic neurons. *Proceedings of the National Academy of Sciences of the USA*, 89, 8462–8466.
- Kusano, K., Fueshko, S., Gainer, H., and Wray, S. (1995). Electrical and synaptic properties of embryonic lutenizing hormone-releasing hormone neurons in explant cultures. *Proceedings of the National Academy of Sciences of the USA*, 92, 3918–3992.
- Mellon, P., Windle, J., Goldsmith, P., Padula, C., Roberts, J., and Weiner, R. (1990). Immortalization of hypothalamic GnRH neurons by genetically targeted tumorigenesis. *Neuron*, 5, 1–10.
- Rehm, H. and Tempel, B. (1991). Voltage-gated  $k^+$  channels of the mammalian brain. *FASEB J.*, 5, 164–170.
- Reinecke, I. and Deuffhard, P. (2007). A complex mathematical model of the human menstrual cycle. *Journal of Theoretical Biology*, 247, 303–330.
- Sim, J., Skynner, M., and Herbison, A. (2001). Heterogeneity in the basic membrane properties of postnatal gonadotropin-releasing hormone neurons in the mouse. *The Journal of Neuroscience*, 21, 1067–1075.
- Stojilkovic, S., Krsmanovic, L., Spergel, D., and Catt, K. (1994). GnRH neurons: intrinsic pulsatility and receptor-mediated regulation. *Trends in Endocrinology and Metabolism*, 5, 201–209.
- Suter, K., Wuarin, J., Smith, B., Dudek, F., and Moenter, S. (2000). Whole-cell recordings from preoptic/hypothalamic slices reveal burst firing in gonadotropin-releasing hormone neurons identified with green fluorescent protein in transgenic mice. *Endocrinology*, 141, 3731–3736.
- Talavera, K. and Nilius, B. (2006). Biophysics and structure-function relationship of T-type  $Ca^{2+}$  channels. *Cell Calcium*, 40, 97–114.
- Tan, S., Farhi, J., Homburg, R., and Jacobs, H. (1996). Induction of ovulation in clomiphene-resistant polycystic ovary syndrome with pulsatile GnRH. *Obstet Gynecol*, 88, 221–6.
- Van Goor, F., Krsmanovic, L., Catt, K., and Stojilkovic, S. (1999). Control of action potential-driven calcium influx in gt1 neurons by the activation status of sodium and calcium channels. *Molecular Endocrinology*, 13, 587–603.
- Watanabe, M., Sakuma, Y., and Kato, M. (2004). High expression of the R-type voltage-gated  $Ca^{2+}$  channel and its involvement in  $Ca^{2+}$ -dependent gonadotropin-releasing hormone release in GT1-7 cells. *Endocrinology*, 145, 2375–2388.
- Zinaman, M., Cartledge, T., Tomai, T., Tippett, P., and Merriam, G. (1995). Pulsatile GnRH stimulates normal cyclic ovarian function in amenorrheic lactating postpartum women. *Journal of Clinical Endocrinology and Metabolism*, 80, 2088–93.